Available online at www.sciencedirect.com
SCIENCE DIRECT
Journal of Catalysis 235 (2005) 201–208
JOURNAL OF CATALYSIS
www.elsevier.com/locate/jcat

Possible reasons for the superior performance of zeolite-based catalysts in the reduction of nitrogen oxides

Meijun Li, Younghoon Yeom, Eric Weitz, Wolfgang M.H. Sachtler *

Department of Chemistry and Institute for Environmental Catalysis, Northwestern University, Evanston, IL 60208, USA

Received 21 April 2005; revised 21 June 2005; accepted 23 June 2005

Abstract

Literature data and results obtained in this laboratory are used to compare catalysts supported on either zeolites or amorphous oxides and used in NO_x reduction to N_2. The data show that the catalytic activity of the zeolite-based materials is higher if alkanes, alkenes, or organic oxygenates are used as reductants, but with ammonia the performance of both groups of catalysts is comparable. These findings are rationalized in the context of the present knowledge of the mechanism of NO_x reduction. Transition metals form oxo-ions on zeolites, but solid solutions on alumina. On zeolites, optimal Coulomb stabilization can be achieved if heterolytic dissociation of molecules transforms multipositive cations to monopositive cations. N_2O_4 dissociates to form $NO^+ + NO_3^-$ on BaNa/Y. In contrast, no NO^+ ions are detected on $BaO/\gamma\text{-}Al_2O_3$. Another important parameter is the high heat of adsorption of small molecules in the narrow zeolite pores. Because oxygenates are superior to alkanes in competing against water for active sites, NO_x reduction with alkanes is favored by zeolites with low Al/Si ratios, but NO_x reduction with acetaldehyde is more efficient on a faujasite with a high Al/Si ratio. Over these catalysts, water vapor actually enhances NO_x reduction by preventing formation of crotonaldehyde, which would poison catalyst sites.

Keywords: De-NO_x catalysis; Zeolites; Competitive adsorption; Charge dissipation

1. Introduction

The introduction of zeolites in catalytic cracking and reforming has had a major impact on the petroleum industry [1]. One motivation for replacing traditional alumina and silica–alumina catalysts by zeolites in this field is their superior acidity in the H form. Zeolites have also been used as catalysts for other processes. A prominent example is H-ZSM-5, a zeolite of MFI structure and an excellent catalyst for the conversion of methanol to high-octane gasoline in Mobil's MTG process. For this application, the geometry of the MFI structure is crucial [2]. The same holds for the selectivity of acid zeolites for direct xylene isomerization toward the *para*-isomer [3]. More recently, superior zeolite-based catalysts have been reported for the one-step oxidation of benzene to phenol [4]. In this case, the propensity of zeolites to favor formation of oxo-complexes, such as ferryl groups, appears to be crucial [5]. Silicalite, a material with the same structure as MFI zeolites, has been identified as an optimal support for the formation of hydrogen peroxide over Ti ions and for the synthesis of epoxides [6].

In the field of selective catalytic reduction (SCR) of nitrogen oxides to nitrogen, zeolite-based materials such as Cu/MFI [7,8], Fe/MFI [9–11], Co/MFI [12,13], and Ba/Y [14,15] are known to display both high activity and selectivity. However, because their thermal stability is inferior to $\gamma\text{-}Al_2O_3$, TiO_2, or ZrO_2 supports, their efficacy in "on board" applications for abating toxic exhaust emissions from cars and diesel trucks is uncertain, although high performance under laboratory conditions has been well established. Thus catalysts have been tested that use the same metal ions on nonzeolitic oxide supports, but these catalysts were often found to be less active for NO_x reduction. Bethke et al. [16] tested Al_2O_3 supported V, Cr, Mn, Fe, Co, Ni, Cu, and Zn

* Corresponding author.
E-mail address: wmhs@northwestern.edu (W.M.H. Sachtler).

0021-9517/$ – see front matter © 2005 Published by Elsevier Inc.
doi:10.1016/j.jcat.2005.06.022

catalysts for NO_x reduction with ethylene, and compared them with catalysts that have the same metal ions in the cavities of an MFI zeolite. These authors report that the temperature at which the catalysts achieve their maximum conversion to N_2 is significantly higher for the γ-Al_2O_3-supported catalysts than for the MFI-supported systems. This finding implies superior activity for the zeolite-based systems. Only zinc catalysts reach their activity maximum at almost the same temperature (near 600 °C) for either support. Because it is well known that transition metal ions form aluminates or solid solutions with γ-Al_2O_3 at high temperature [17], these authors wondered whether the superior performance of the zeolite-supported catalysts could be due to a better maintenance of the original dispersion of the active ions.

Because SCR catalysts are usually tested in flow reactors under conditions where the temperature is increased in an atmosphere with a large excess of O_2 over NO_x, it is useful to remember that the shapes of plots of the N_2 yield versus temperature reflect a competition between two reactions. At low temperature, the reductant reacts mainly with NO_2 or N_2O_3 [18] in a sequence of steps leading to the production of N_2. At high temperature, however, the thermodynamically preferred combustion of organic reductants with O_2 prevails. Likewise, if ammonia is used as the reductant, then its oxidation to NO becomes significant at high temperature. For all of these reductants, the N_2 yield will ultimately decrease with temperature. Thus, one can argue that the *activity* of de-NO_x catalysts for the desired reaction can be defined by their "light off" temperature and the early part of the *ascending* branch of the N_2 yield-versus-T plot, whereas the yield maximum reflects the point at which the undesired combustion process starts to win out over the desired reaction because of limited *selectivity* for the latter process.

If different resistance against the interaction of the active ion with the support were the only cause of the different effects of zeolite and non-zeolite supports, then one would expect to find similar performance with either support at low temperature. In the present work we tested this hypothesis by comparing the N_2 yield over different catalysts, not only at their yield maximum, but also in the low-temperature regime, where other causes, such as differences in physisorption, the presence or absence of an electric field in the cavities of the support, and/or different energies of charge separation might affect the impact of the support on catalytic performance.

We compared literature data and results measured in our laboratory for NO_x reduction to N_2 with the following reductants: propane, isobutane, propene, ethanol, acetaldehyde, and ammonia. The zeolite-based catalysts are Cu/MFI, Cu/Mor, Fe/MFI, Co/MFI, Ag/Y, and BaY (or BaNa/Y). We compare the performance over these catalysts with the performance over Cu/TiO_2, Cu/ZrO_2, Co/γ-Al_2O_3, Ag/γ-Al_2O_3, Ba/γ-Al_2O_3, and Ba/TiO_2. We compare the temperatures at which the maximum N_2 yield and a lower yield (20% in most cases) are achieved with catalysts with the same active element supported on different carriers. Not all literature data were measured at the same space velocity and/or with the same feed composition; we use such data only if differences between catalysts with different supports are large.

2. Experimental

Here we describe the procedure for catalysts prepared in our laboratory. For catalysts used by other authors, refer to their papers.

Briefly, 5.5 wt% BaNa/Y was obtained by a three-fold ion exchange of Na/Y (Si/Al = 2.5, Aldrich) with an aqueous 0.1 mol $Ba(NO_3)_2$ solution. For the preparation of 2 wt% Ag/Y, an $AgNO_3$ solution was used at ambient temperature. After every exchange, the slurry was stirred for 48 h before vacuum-filtered, washed thoroughly with double-deionized H_2O, and dried in air. The alumina-supported catalysts 4 wt% Ag/γ-Al_2O_3, 5.5 wt% Ba/γ-Al_2O_3, and 5.5 wt% Ba/TiO_2 were prepared by wet impregnation.

We recorded in situ Fourier transformed infrared spectra in transmission mode with a Bio-Rad Excalibur FTS-3000 infrared spectrometer equipped with a MCT detector. Unless otherwise stated, we obtained each spectrum by averaging 70 scans at a resolution of 2 cm^{-1}. The "homemade" infrared cell, described in more detail in [15], is based on the design in [19] and comprises a stainless-steel cube with two CaF_2 windows that can be pumped differentially. A fresh catalyst sample was used for each new set of experiments.

We carried out catalytic tests in a fixed-bed microflow reactor, described in more detail in [20]. Briefly, 0.2 g of the powdered catalyst was packed into the quartz reactor. The composition of the feed gas was regulated by mass-flow controllers (URS-100, UNIT Instruments). H_2O was introduced into the reaction system by bubbling He through a H_2O saturator. The composition of the effluent was analyzed "on-line" with a gas chromatograph (GC) equipped with a thermal conductivity detector (TCD) (5A column for N_2 and CO, Porapak Q for CO_2). A cold trap was positioned between the reactor and the GC to protect the column from H_2O.

3. Results

Fig. 1a shows data for the reduction of NO_2 with acetaldehyde over BaNa/Y as a function of the reaction temperature with a feed containing 2% water. The maximum N_2 yield is obtained at 200 °C. Kung et al. [21] reported that over TiO_2, this maximum is obtained at $T > 300$ °C. Fig. 1b shows our results for the same reaction over BaO/γ-Al_2O_3 and BaO/TiO_2. In agreement with the results of Kung [21], the temperature of maximum N_2 yield is >300 °C for both catalysts. The temperature at which a 20% N_2 yield is registered is 95 °C for BaNa/Y, but a much higher temperature is

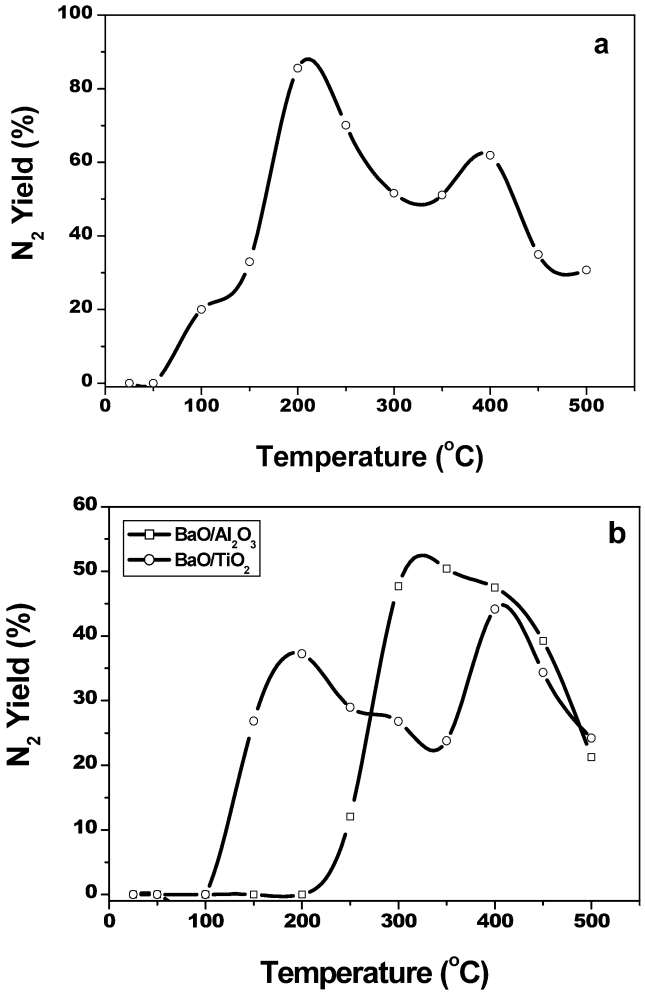

Fig. 1. NO_2 reduction with acetaldehyde in a wet feed as a function of reaction temperature over (a) Ba,Na/Y, (b) BaO/γ-Al_2O_3 and BaO/TiO_2. AA, 500 ppm; NO_2, 500 ppm; O_2, 7.0%; H_2O, 2.0%; total flow rate, 200 ml/min; 0.2 g catalyst.

Table 1
$NO_x + CH_3CHO$; Ba sites

Catalyst	T at 20% yield (°C)	T at max. yield (°C)	Y_{max} (%)	Ref.
Ba,Na/Y	95	200	90	This work
BaO/γ-Al_2O_3	250	315	51	This work
BaO/TiO_2	135	400	45	This work

Table 2
$NO_x + C_2H_5OH$; Ag sites

Catalyst	T at 20% yield (°C)	T at max. yield (°C)	Y_{max} (%)	Ref.
Ag/Y	70	290	83	This work
Ag/γ-Al_2O_3	180	350	100	This work

required for BaO on γ-Al_2O_3 or TiO_2; the relevant parameters are given in Table 1.

Fig. 2 shows NO_2 reduction with ethanol in a wet feed, as a function of reaction temperature, over Ag/γ-Al_2O_3 and

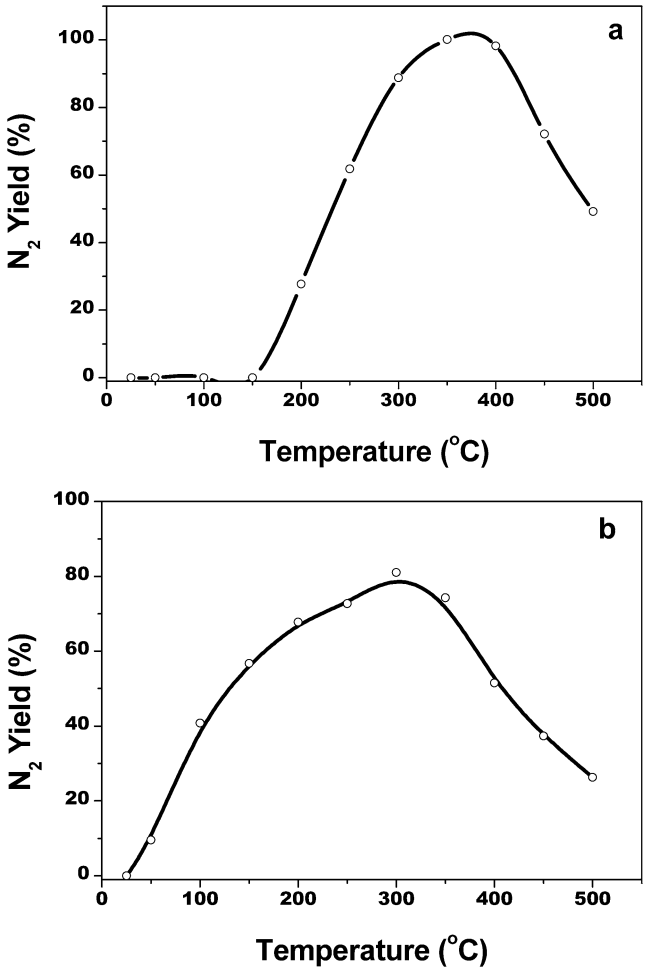

Fig. 2. NO_2 reduction with ethanol in a wet feed as a function of reaction temperature over (a) Ag/γ-Al_2O_3 and (b) AgY. Ethanol, 1000 ppm; NO_2, 500 ppm; O_2, 7.0%; H_2O, 2.0%; total flow rate: 200 ml/min, 0.2 g catalyst.

Table 3
$NO_x + C_3H_6$; Co sites

Catalyst	T at 20% yield (°C)	T at max. yield (°C)	Y_{max} (%)	Ref.
Co/MFI[a]	310	350	83	[22]
Co/Al_2O_3[b]	400	460	78	[22]

[a] 0.095% NO, 0.1% C_3H_6, 5% O_2 and 1.7% H_2O; total flow rate, 100 ml/min; 0.5 g 1.24 wt% Co/MFI.

[b] 0.095% NO, 0.1% C_3H_6, 5% O_2 and 1.7% H_2O; total flow rate, 100 ml/min; 0.5 g 2 wt% Co/Al_2O_3.

Ag/Y; the relevant parameters are given in Table 2. Clearly, a much higher temperature is required to attain both the 20% yield point and the maximum N_2 yield over Ag/γ-Al_2O_3 than over Ag/Y. The required temperature for the 20% yield point for Ag/γ-Al_2O_3 is 110 °C higher than that for Ag/Y. All of these criteria indicate a superior activity for the zeolite-supported catalysts.

For the SCR of NO_x with propene, we again compare (in Table 3) the temperature at which the catalysts reach the 20% yield point [22]. This temperature is 90 °C lower

Table 4
$NO_x + C_2H_4$; sites Fe

Catalyst	T at 20% yield (°C)	T at max. yield (°C)	Y_{max} (%)	Ref.
Fe-MOR-97[a]	250	250	20	[27]
FeO/Al_2O_3[b]	400	400	21	[27]

[a] NO, 1000 ppm; C_2H_4, 250 ppm; O_2, 2%; and W/F, 0.2 g s cm^{-3}.
[b] NO, 1000 ppm; C_2H_4, 250 ppm; O_2, 2%, and W/F, 0.2 g s cm^{-3}.

Table 5
NO_x + NH_3, Cu sites

Catalyst	T at max. yield (°C)	Y_{max} (%)	T at 50% yield (°C)	Ref.
Cu/MOR[a]	240	100	180	[29]
CuO/ZrO_2[b]	300	35	–	[30]
CuO/TiO_2[b]	220	95	180	[30]

[a] NO, 500 ppm; NH_3, 500 ppm; O_2, 5%; GHSV, 100,000/h; 2.3 wt% Cu/MOR.
[b] NO, 35 ml/min; NH_3, 35 ml/min; air, 1350 ml/min; GHSV, 20,000/h.

over Co/MFI than over Co/γ-Al_2O_3. Though the maximum yields are comparable, the zeolite-based catalyst achieves this yield at a temperature that is also 90 °C lower than for the Co/γ-Al_2O_3 catalyst.

Supported iron catalysts have been used in the SCR of NO_x. High yields are achieved with isobutane over Fe/MFI [23–26]. As is evident from Table 4, with ethylene a much higher temperature is required over γ-Al_2O_3-supported Fe catalysts than over Fe/Mor for both the 20% yield point and the maximum yield [27].

Although there are data for SCR with propane over Fe/MFI [11], Co/γ-Al_2O_3 [22], and Cu/MFI [28] catalysts, comparisons are problematic because different space velocities have been used. Nonetheless, the data show that much higher temperatures for both the maximum yield and the 20% yield are required for Co/γ-Al_2O_3 than for Fe/MFI or Cu/MFI.

Reduction of NO_x with ammonia has been studied by numerous authors [29,30]. Table 5 presents literature data obtained with Cu supported on mordenite, titania, and zirconia. The highest yield, of 95%, is found for CuO/TiO_2 at 220 °C and Cu/MOR at 240 °C; the 50% yields are registered at approximately the same temperature over both catalysts. It is not clear, and not within the scope of this paper, to consider, why the TiO_2 and ZrO_2 supports behave differently. Sun et al. reported that over Fe/MFI ammonia, conversion to N_2 exceeds 70% at 275 °C and reaches 90% at 300 °C. Clearly, very high N_2 yields are possible with ammonia over both zeolite-supported and TiO_2-supported transition metal catalysts.

The totality of these results suggests that for NO_x reduction with organic reductants, the zeolite-supported catalysts are more active than catalysts using the same ions on other supports. But when ammonia is used as the reductant, catalytic performance is comparable for zeolitic and nonzeolitic supports.

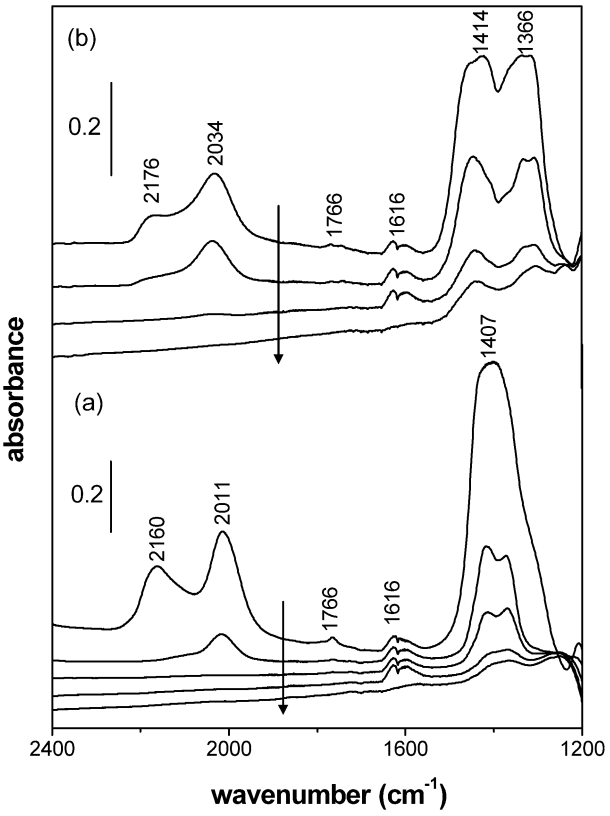

Fig. 3. FTIR spectra after exposure of Na-Y (a) and BaNa/Y (b) to 1 Torr of NO_2. Each sample was activated at 430 °C for 3 h in vacuum before the NO_2 was admitted to the cell. For both top to bottom (as indicated by the arrows) panels, the spectra were taken at 50, 100, 150, and 200 °C, and after subsequent evacuation. The temperature was increased at a rate of 2.5 °C/min.

To rationalize these findings, it is useful to consider the adsorption complexes that have been identified through IR spectroscopy. Fig. 3a shows a series of FTIR spectra recorded after exposing Na/Y to NO_2. Absorption bands at 2011 and 2160 cm^{-1} are due to NO^+ ions formed by the reaction

$$N_2O_4\ (\rightleftarrows 2NO_2) \rightarrow NO^+_{ads} + NO_{3ads}^-.$$

Details of this reaction have been reported elsewhere [15,31]. The nitrate counter ion for NO^+ is initially observed as a strong absorption band at 1407 cm^{-1} (see the top trace). Increasing the temperature causes this band to split into two bands, at 1370 and 1415 cm^{-1}. Fig. 3b shows a series of FTIR spectra recorded by exposing BaNa/Y to NO_2. The absorption bands at 2034 and 2176 cm^{-1} are due to the NO^+ ions, that is, the co-product of dissociative chemisorption of N_2O_4. These bands are shifted to higher energy on BaNa/Y than on Na/Y (∼23 and ∼16 cm^{-1}, respectively). This indicates that the oxygen anions of the zeolite framework in Ba,Na/Y donate less electron density to NO^+ than those in Na/Y. This result is ascribed to the lower negative charge of the O^{2-} ions in Ba,Na/Y in comparison to Na/Y, because Ba^{2+} ions more strongly attract electrons from their oxygen neighbors than Na^+ ions do. The stretching frequency of

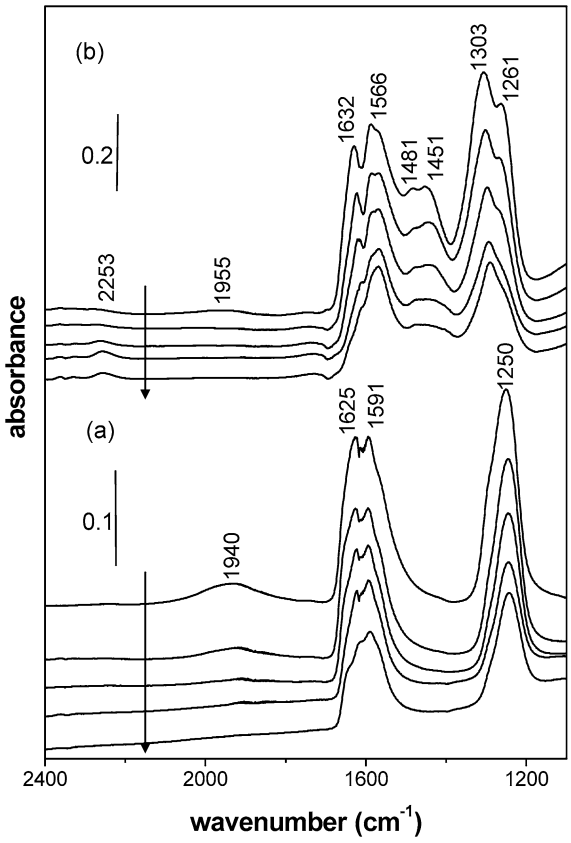

Fig. 4. FTIR spectra after exposure of γ-Al_2O_3 (a) and BaO/γ-Al_2O_3 (b) to 1 Torr of NO_2. Each sample was activated at 430 °C for 3 h in vacuum before the NO_2 was admitted to the cell. For both top to bottom (indicated by the arrows) panels, the spectra were taken at 50, 100, 150, and 200 °C, and after subsequent evacuation. The temperature was increased at a rate of 2.5 °C/min.

NO^+ varies with the nature of the cation because it depends on the degree of electron transfer from the anion to the π^* orbital of NO^+. Nitrate ions on BaNa/Y are characterized by strong absorption bands at 1366 and 1414 cm^{-1} (see the top trace). For both catalysts, the bands centered at 1616 and 1766 cm^{-1} are due to gas phase NO_2 and the $\nu_1 + \nu_2$ combination band of NO_3^-, respectively. The thermal stability of NO^+ is different for Na/Y and BaNa/Y. Raising the temperature from 56 to 100 °C causes the intensity of the band for NO^+_{ads} on BaNa/Y to decrease by 7%, and that of NO^+_{ads} on Na/Y to decrease by 84%. At 200 °C, no NO^+_{ads} band can be detected on Na/Y, but on BaNa/Y the NO^+ band remains clearly detectable (although not on the absorbance scale used in this figure). We conclude that the concentration of NO^+_{ads} is higher at 200 °C on BaNa/Y than on Na/Y. When the temperature is raised from 50 to 200 °C, the intensity of the nitrate bands on BaNa/Y decreases by ∼84% and that for the bands on Na/Y decreases by ∼96%. This indicates that the thermal stability of nitrates is higher in the presence of exchanged Ba^{2+} ions.

Fig. 4 compares γ-Al_2O_3 and BaO/γ-Al_2O_3. Panels (a) and (b) show the FTIR spectra after exposure to NO_2. Strong bands appear immediately at 1250, 1591, and 1625 cm^{-1}

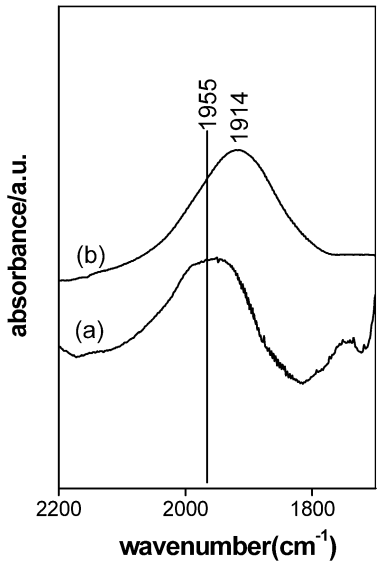

Fig. 5. FTIR spectra after exposure of BaO/γ-Al_2O_3 to 1 Torr of NO_2 (a) and $^{15}NO_2$ (b) at 50 °C.

(see the top trace in (a)). Based on literature data, these bands are assigned to bridging bidentate nitrates [32–34]. There are more bands on BaO/γ-Al_2O_3 than on γ-Al_2O_3 (see (b)), because in the former system two solid phases, BaO and γ-Al_2O_3, coexist. The features at 1303, 1451, and 1481 cm^{-1} are due to ionic nitrates formed on BaO. The bands at 1261 and 1632 cm^{-1} are assigned to bridging bidentate nitrate [ν(N=O) and $\nu_{asym}(NO_2)$] on BaO/γ-Al_2O_3. The band at 1566 cm^{-1} is ascribed to bridged chelating bidentate nitrate on BaO. A broad absorption band at 1940 cm^{-1} on γ-Al_2O_3 and at 1955 cm^{-1} on BaO/γ-Al_2O_3 gradually decreases in intensity with upon increasing temperature and can hardly be seen at 200 °C. Ba/γ-Al_2O_3 was exposed to $^{15}NO_2$ to check whether the 1955 cm^{-1} band shifted. Indeed, it did shift (by ∼41 cm^{-1}) to a lower frequency with $^{15}NO_2$ (Fig. 5). This band is probably due to the interaction of $NO_2^{\delta+}$ and Al^{3+}. A similar band has been observed at ∼1970 cm^{-1} when γ-Al_2O_3 was exposed to NO + O_2 [32]. This band has been assigned to $NO_2^{\delta+}$ interacting with Al^{3+} [32]. No NO^+ bands are observed between 2000 and 2400 cm^{-1} with the sensitivity scale used here. If any NO^+ ions were formed on this catalyst, their concentrations were orders of magnitude lower than on the zeolite-based catalysts BaNa/Y and Na/Y. This indicates that dissociative chemisorption of N_2O_4 to $NO^+ + NO_3^-$ is much less on alumina than on the zeolite-based catalysts.

An absorption band at 2253 cm^{-1} is observed with BaO/γ-Al_2O_3 but not with γ-Al_2O_3. This band becomes stronger with increasing temperature (Fig. 4a) and does not shift when BaO/γ-Al_2O_3 is exposed to $^{15}NO_2$. The assignment of this band is beyond the scope of this paper. If the extinction coefficients for adsorbed nitrates in the 1100–1700 cm^{-1} region are similar for BaO/γ-Al_2O_3 and γ-Al_2O_3, then it follows from the integrated absorbances at 50 °C that the concentration of nitrate is roughly 2.5 or-

ders of magnitude higher on $BaO/\gamma\text{-}Al_2O_3$ than on Al_2O_3. Raising the temperature from 50 to 200 °C decreases the integrated absorbance by ∼56% for both solids; however, the overall intensity of adsorbed nitrate in this region at 200 °C is still ∼2.5 times higher on $BaO/\gamma\text{-}Al_2O_3$.

For BaNa/Y, the dissociation of N_2O_4 is an important source of adsorbed NO_3^- ions. But for the alumina-based catalysts, this route is apparently unavailable; as previously proposed, a major path is

$$BaO + 3NO_2 \rightarrow Ba(NO_3)_2 + NO. \quad (1)$$

Despres et al. [35] studied the forward and reverse reactions in Eq. (1) on BaO/TiO_2 using TPD. They observed that NO_2 consumption and NO production in the forward reaction occur in a 3:1 ratio. They also observed the reverse process, that is, reduction of the nitrate with NO. As mentioned in Ref. [32], formation of nitrate from NO_2 is also possible through BaO_2.

4. Discussion

The catalytic data show that with alkanes, alkenes, or oxygenates as reductants, the NO_x reduction activity of zeolite-supported catalysts is superior to that of catalysts using conventional nonzeolitic oxides as the support. Both the maximum yield and the yield measured at low conversion support this conclusion.

Before discussing possible reasons for this difference in performance, we briefly recapitulate our present understanding of the reaction mechanism for NO_x reduction. Isotopic labeling clearly shows that in each N_2 molecule formed by SCR, one of the N atoms stems from a precursor in which it had the formal oxidation state of −3, as in NH_3, and the other N atom had an oxidation number of +3, as in N_2O_3 [18,36–38]. N_2 formation thus occurs in a process for which the decomposition of ammonium nitrite is the prototype,

$$NH_4NO_2 = N_2 + 2H_2O. \quad (2)$$

As was found with aqueous solutions of NH_4NO_2 by Millon in 1847 [39] and with NH_4NO_2 deposited on quartz by Li et al. [40], this decomposition is rapid near 100 °C and does not require a catalyst. For the SCR of NO_x with ammonia, the highest yield of N_2 is *always* obtained if NO and NO_2 are present in a 1/1 ratio. A catalyst can facilitate formation of this ratio by increasing the rate of either the forward or the backward reaction,

$$2NO + O_2 \rightleftarrows 2NO_2. \quad (3)$$

For reductants other than ammonia or an amine, the reductant must first reduce part of the NO_x to NH_3, as was first suggested by Poignant et al. [41]. This ammonia will then react with the remaining NO_x [15]. Conversion of part of the NO_x to ammonia has been studied in considerable detail for BaNa/Y catalysts using acetaldehyde as the reductant [15]. In brief, the acetaldehyde is first oxidized by NO_2 to acetic acid. The acetate ions exchange their carboxylate group with NO_2, yielding the acid-form of nitromethane. This intermediate is subsequently dehydrated (probably through a pathway involving formo-hydroxamic acid) to isocyanic acid, which then reacts with water

$$CH_3NO_2 \rightarrow HNCO + H_2O \rightarrow CO_2 + NH_3. \quad (4)$$

Considering the reaction mechanism along with data on the efficiency of different catalytic systems for reducing NO_x to N_2, it appears that zeolite's special role is manifested in the reduction of NO_x to NH_3 and that zeolite has less effect on the subsequent steps. To rationalize these findings, we consider three characteristic propensities that distinguish zeolites from other solid oxides:

1. Selective oxidation is preferred on isolated oxo-ions, such as $[Cu–O–Cu]^{2+}$ or $[FeO]^+$, in zeolites, but nonselective combustion is preferred on oxide particles or their solid solutions. This aspect is crucial for the *selectivity* of catalysts containing transition metal ions. But since this paper focuses on the effects of the support on the *activity* of the catalysts, with special emphasis on catalysts that do not contain transition metal ions, this aspect is not pursued further here.
2. Dissociative chemisorption of molecules such as H_2O (to $H^+ + OH^-$) or N_2O_4 (to $NO^+ + NO_3^-$) is energetically preferred on zeolites with multipositive cations in their cavities.
3. The heat of physisorption of many molecules is higher in the nanopores of a zeolite than on amorphous oxides.

We now discuss points 2 and 3 in more detail. For point 2, a characteristic of zeolite structure is that the negative charge is effectively localized on Al-centered oxygen tetrahedra in the rigid lattice, but the positive-charge carriers are ions located in the cavities. Only the positive-charge carriers are mobile. For mono-positive ions, such as Na^+, it is obvious that Coulomb interactions will be optimum when the positive ions are positioned near the negative-charge carriers. But for multipositive ions, such as Ba^{2+} and Ga^{3+}, a compromise position must be found for the positive-charge carrier, because it cannot simultaneously be a close neighbor of each of the two or three immobile negative charges that it compensates. In this situation the Coulomb energy of the system will be lowered by adsorbates that dissipate the $(n+)$ charge of the positive ion into $n(1+)$ charges that can seek positions near an Al-centered tetrahedron of the zeolite.

Examples of such charge dissipation are hydrolysis reactions, such as

$$Ga^{3+} + H_2O = [GaO]^+ + 2H^+. \quad (5)$$

In the case of BaNa/Y, the results of this paper show that charge dissipation is achieved by the dissociative chemisorption of N_2O_4,

$$N_2O_4 + Ba^{2+} = [Ba–NO_3]^+ + [NO]^+, \quad (6)$$

which effectively transforms a 2+ charge carrier into two mobile 1+ charged carriers. The IR results in this paper demonstrate that the $[NO]^+$ ions formed in this process on BaNa/Y exhibit a fairly strong IR band, but no such band is detectable with BaO/γ-Al_2O_3 or γ-Al_2O_3. Because the $[NO]^+$ ion is known to form nitrous acid (HONO) on reaction with water, its presence provides a path for the formation of ammonia nitrite. This path may be less important in the presence of a high partial pressure of ammonia, because reduction of nitrate ions to nitrite ions provides another efficient route toward ammonia nitrite. However, for catalytic reactions where ammonia must be formed by NO_x reacting with an organic molecule, nitrite formation through hydration of the $[NO]^+$ ion is likely to become dominant, because the concentration of ammonia will be low in the steady state.

In terms of point 3, the third characteristic difference between zeolite and nonzeolite supports is the heat of physisorption in the pores of the support. Data obtained by calorimetry or derived from isosteric equilibria have been reported by various authors, including Breck [42] and Stach et al. [43]. Using silicalite analogs of MFI and FAU lattices, Eder and Lercher [44] showed that the heat of adsorption of *n*-hexane depends strongly on the pore diameter, being >70 kJ/mol on MFI but only 45 kJ/mol on FAU. When discussing the consequences of adsorption on the effectiveness of SCR catalysts, one must consider that actual de-NO_x processes always occur in the presence of a partial pressure of water exceeding that of the organic reductant or ammonia. Adsorption of the reductant thus must compete with adsorption of water on the same sites. Work focusing on this *competitive* adsorption has been published by Hunger et al. [45], who used temperature-programmed desorption to determine the activation energy, E_{des}, which will be very similar to the enthalpy of adsorption. These authors showed that methanol displaces adsorbed water from the strongest adsorption sites of Na/MFI. The E_{des} of methanol is 75–100 kJ/mol. This finding explains why oxygenates such as acetaldehyde or ethanol can achieve NO_x reduction in the presence of water vapor at a lower temperature than alkanes, which also require that a transition metal oxo-complex be partially oxidized.

The concept of competitive adsorption of reductant and water is illustrated by the well-known negative effect of water vapor on the NO_x reduction rate over such catalysts as Cu/MFI and Co/MFI. It is, therefore, quite remarkable that water vapor has a much less inhibiting effect when an oxygenate is used as the reductant. In the case of NO_x reduction with acetaldehyde over BaNa/Y, our data show *higher* NO_x conversion in the presence of water than in its absence [20]. This remarkable result has been rationalized by considering that the presence of water will shift the equilibrium for aldol condensation (7) to the left, thus minimizing the formation of crotonaldehyde, which is a potential precursor of coke that deactivates catalyst sites:

$$2CH_3CHO = CH_3\text{–}CH{=}CH\text{–}CHO + H_2O. \quad (7)$$

We conclude that enhanced adsorption of the reductant and formation of NO^+ ions are likely causes of the superior activity of zeolite-based de-NO_x catalysts. Because adsorption of the reducing agent occurs in competition with water vapor, one can understand that for nonpolar hydrocarbons, the "hydrophobic" zeolites [46] with low Al/Si ratio are optimum, but with polar molecules, such as acetaldehyde or ethanol, high N_2 yields are obtained at lower temperatures over "hydrophilic" zeolites with high Al/Si ratios.

Acknowledgments

This research was supported by the Chemical Sciences, Geosciences and Biosciences Division, Office of Basic Energy Sciences, Office of Science, US Department of Energy (Grant No. DE-FG02-03ER15457). The authors thank the donors of the American Chemical Society Petroleum Research Fund for their partial support of this work and Professor R. Snurr for his helpful suggestions.

References

[1] H. Heinemann, in: G. Ertl, H. Knözinger, H. Weitkamp (Eds.), Handbook of Heterogeneous Catalysis, vol. 1, Chemie, Weinheim, Germany, 1997, pp. 35–48.
[2] S.L. Meisel, J.P. Mc Cullough, C.H. Lechthaler, P.B. Weia, Chem. Tech. 6 (1976) 86.
[3] S.M. Csicsery, Zeolites 4 (1984) 202–213.
[4] G.I. Panov, A.S. Kharitonov, V.I. Sobolev, Appl. Catal. A 98 (1993) 1.
[5] K.A. Dubkov, N.S. Ovanesyan, A.A. Shteinman, E.V. Starokon, G.I. Panov, J. Catal. 207 (2002) 341.
[6] B. Notari, Adv. Catal. 41 (1996) 253.
[7] M. Iwamoto, H. Yhiro, Y. Yu-U, S. Shundo, N. Mizuno, Sholubai 32 (1990) 430.
[8] J. d' Itri, W.M.H. Sachtler, Catal. Lett. 15 (1992) 289.
[9] X. Feng, K. Hall, Catal. 166 (1997) 368.
[10] H.-Y. Chen, W.M.H. Sachtler, Catal. Today 42 (1998) 73.
[11] H.-Y. Chen, T. Voskoboinikov, W.M.H. Sachtler, Catal. Today 54 (1999) 483.
[12] Y. Li, J.N. Armor, Appl. Catal. B 1 (1992) L31.
[13] X. Wang, H.-Y. Chen, W.M.H. Sachtler, Appl. Catal. B 19 (2001) 47.
[14] G. Panov, R.G. Tonkyn, M.L. Balmer, C.H.F. Peden, SAE 2001 01-3513.
[15] Y.H. Yeom, B. Wen, W.M.H. Sachtler, E. Weitz, J. Phys. Chem. B 108 (2004) 5386.
[16] K.A. Bethke, M.C. Kung, B. Yang, M. Shah, D. Alt, C. Li, H.H. Kung, Catal. Today 26 (1995) 169.
[17] P.H. Bolt, Transition metal aluminate formation in alumina supported model catalysts, thesis, University of Utrecht, The Netherlands, 1994.
[18] Q. Sun, Zh.-X. Gao, H.-Y. Chen, W.M.H. Sachtler, J. Catal. 201 (2001) 89.
[19] P. Basu, T.H. Ballinger, J.T. Yates, Rev. Sci. Instrum. 59 (1988) 1321.
[20] B. Wen, Y.H. Yeom, E. Weitz, W.M.H. Sachtler, Appl. Catal. B 48 (2004) 125.
[21] A.P. Kozlova, H.Y. Law, M.C. Kung, H.H. Kung, Catal. Lett. 95 (2004) 211.
[22] J.Y. Yan, M.C. Kung, W.M.H. Sachtler, H.H. Kung, J. Catal. 172 (1997) 178.
[23] H.-Y. Chen, W.M.H. Sachtler, Catal. Today 42 (1998) 73.
[24] T.V. Voskoboinikov, H.-Y. Chen, W.M.H. Sachtler, Appl. Catal. B 19 (1998) 275.

[25] H.-Y. Chen, T. Voskoboinikov, W.M.H. Sachtler, J. Catal. 186 (1999) 91.
[26] H.-Y. Chen, X. Wang, W.M.H. Sachtler, Phys. Chem., Chem. Phys. 2 (2000) 3083.
[27] S. Sato, H. Hirabayashi, H. Yahiro, N. Mizuno, M. Iwamoto, Catal. Lett. 12 (1992) 193.
[28] R. Gopalakrishnan, P.R. Stafford, J.E. Davidson, W.C. Hecker, C.H. Bartholomew, Appl. Catal. B 2 (1993) 165.
[29] S.W. Ham, H. Chio, I.S. Nam, Y.G. Kim, Catal. Lett. 42 (1996) 35.
[30] T. Iizuka, H. Ikeda, J. Chem. Soc., Faraday Trans. 1 82 (1986) 61.
[31] Y.H. Yeom, J. Henao, M.-J. Li, W.M.H. Sachtler, E. Weitz, J. Catal. 231 (2005) 181.
[32] F. Prinetto, G. Ghiotti, I. Nova, L. Lietti, E. Tronconi, P. Forzatti, J. Phys. Chem. B. 105 (2001) 12732.
[33] F. Prinetto, G. Ghiotti, I. Nova, L. Castoldi, L. Lietti, E. Tronconi, P. Forzatti, Phys. Chem. Chem. Phys. 5 (2003) 4428.
[34] J. Szányi, J.H. Kwak, D.H. Kim, S.D. Burton, C.H.F. Peden, J. Phys. Chem. B. 109 (2005) 27.
[35] J. Despres, M. Koebel, O. Krocher, M. Elsener, A. Wokaun, Appl. Catal. B. 43 (2003) 389.
[36] H.-Y. Chen, T. Voskoboinikov, W.M.H. Sachtler, J. Catal. 180 (1998) 171.
[37] H.-Y. Chen, T. Voskoboinikov, W.M.H. Sachtler, J. Catal. 186 (1999) 91.
[38] H.-Y. Chen, Q. Sun, B. Wen, Y.-H. Yeom, E. Weitz, W.M.H. Sachtler, Catal. Today 96 (2004) 1.
[39] E. Millon, Ann. Chim. Phys. 19 (1847) 255.
[40] M.-J. Li, J. Henao, Y.-H. Yeom, E. Weitz, W.M.H. Sachtler, Catal. Lett. 98 (2004) 5.
[41] F. Poignant, J. Saussey, J.C. Lavalley, G. Mabilon, Chem. Comm. (1995) 89.
[42] D.W. Breck, Zeolite Molecular Sieves, Structure, Chemistry and Use, Wiley, New York, 1974, p. 654.
[43] H. Stach, U. Lohse, H. Thamm, W. Schirmer, Zeolites 74 (1986) 74.
[44] F. Eder, J.A. Lercher, Zeolites 18 (1997) 7.
[45] B. Hunger, S. Matysik, M. Heuchel, W.-D. Einicke, Langmuir 13 (1997) 6249, J. Thermal Anal. Calorim. 64 (2001) 1183.
[46] D.H. Olson, W.O. Haag, W.S. Borghard, Microporous Mesoporous Mater. 35–36 (2000) 435.